

Magnetism in Multiferroic BiFeO_3

Alim Solmaz

IMS Journal Club Presentation

17-04-2012



Outline

- Reborn of BiFeO_3
- Magnetic Properties
 - Magnetoelectric effect
 - Exchange coupling
- Electrical control of Ferromagnetic domains and device applications
- Conclusion and Outlook
- References

Reborn of BiFeO₃

- High quality single crystal thin films
- G-type Antiferromagnetic Ferroelectric at RT
 - $T_C \sim 870^\circ\text{C}$ and $T_N \sim 370^\circ\text{C}$
- Rhombohedral R3c

Epitaxial BiFeO₃ Multiferroic Thin Film Heterostructures

J. Wang,¹ J. B. Neaton,^{2†} H. Zheng,^{1†} V. Nagarajan,¹ S. B. Ogale,³
 B. Liu,¹ D. Viehland,⁴ V. Vaithyanathan,⁵ D. G. Schlom,⁵
 U. V. Waghmare,⁶ N. A. Spaldin,⁷ K. M. Rabe,²
 M. Wuttig,¹ R. Ramesh^{3*}

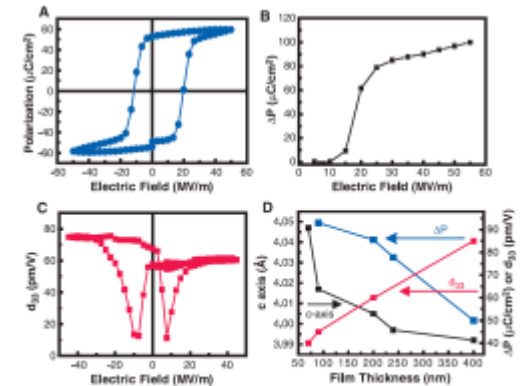
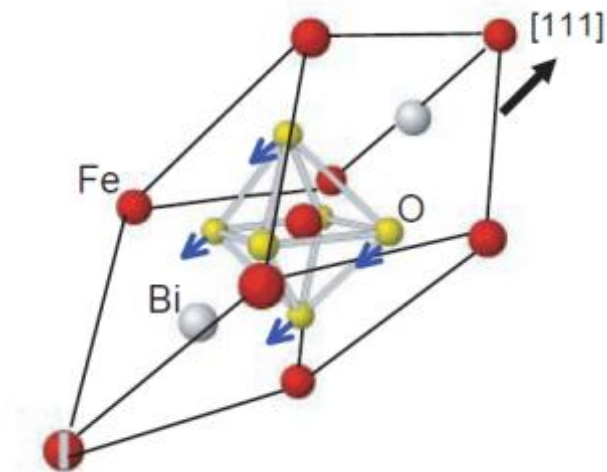


Fig. 2. (A) A ferroelectric hysteresis loop measured at a frequency of 15 kHz, which shows that the film is ferroelectric with $P_r \sim 55 \mu\text{C}/\text{cm}^2$. (B) Pulsed polarization ΔP versus electric field measured with electrical pulses of 10- μs width. (C) A small signal d_{33} for a 50- μm capacitor. (D) A summary of the thickness dependence of out-of-plane lattice parameter, polarization, and d_{33} . The small signal dielectric constant (27) follows the same trend as the d_{33} .



Reborn of BiFeO₃

- Magnetic moment detected (?)

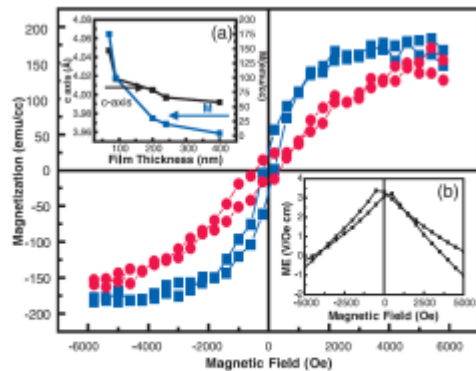
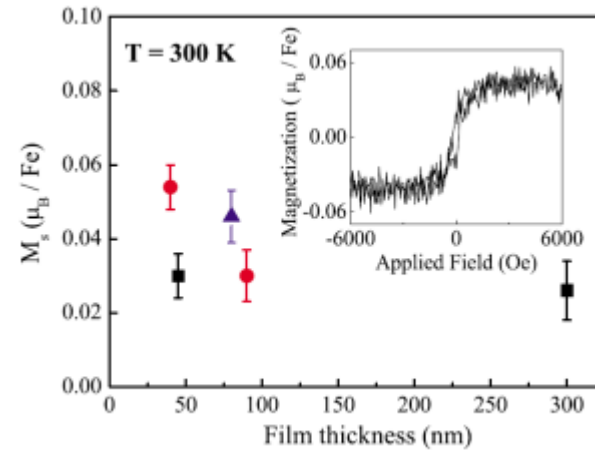


Fig. 4. Magnetic hysteresis loops measured by vibrating sample magnetometry for a 70-nm-thick BFO film, showing an appreciable saturation magnetization of -150 emu/cm^3 and a coercive field of -200 Oe . The in-plane loop is shown in blue, and the out-of-plane loop is in red. Inset (a) shows the thickness dependence of saturation magnetization, illustrating the effect of heterospitaxial constraint. Inset (b) is a preliminary ME measurement result showing a maximum value of -3 V/cm-Oe and hysteresis about 200 Oe .

vs.



Eerenstein et. al. *Science* 307, 1203 (2005)

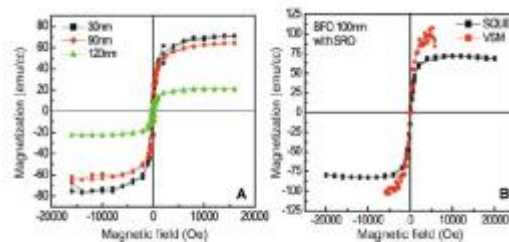
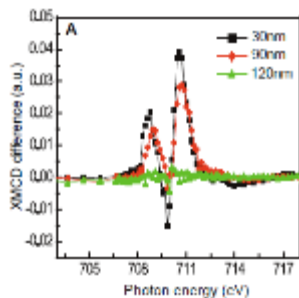


Fig. 1. [A] Magnetic response from BFO films grown on 001 STO with different thickness. [B] Comparison of VSM and SQUID results on the 100-nm BFO/SrO/STO [001] sample used in [2]. Care was taken to remove any silver spots on the substrate by grinding with emery paper.

Magnetic Properties

- Ferromagnetism in ferroelectric domain walls of antiferromagnetic multiferroics

Ferroelectrics, 375:122-131, 2008
 Copyright © Taylor & Francis Group, LLC
 ISSN: 0015-0193 print / 1563-5112 online
 DOI: 10.1080/00150190802437969



Landau Theory of Ferroelectric Domain Walls in Magnetoelectrics

M. DARAKTCHIEV,* G. CATALAN, AND J. F. SCOTT

$$\begin{aligned}
 G_{MP} &= G_0 + \frac{\kappa}{2}(\nabla P)^2 + \frac{\lambda}{2}(\nabla M)^2 + L_{MP}(P, M) \\
 &= G_0 + \frac{\kappa}{2}(\nabla P)^2 + \frac{\lambda}{2}(\nabla M)^2 + \frac{\alpha}{2}P^2 + \frac{\beta}{4}P^4 + \frac{\eta}{6}P^6 + \frac{a}{2}M^2 \\
 &\quad + \frac{b}{4}M^4 + \frac{n}{6}M^6 + \frac{\gamma}{2}P^2M^2
 \end{aligned}$$

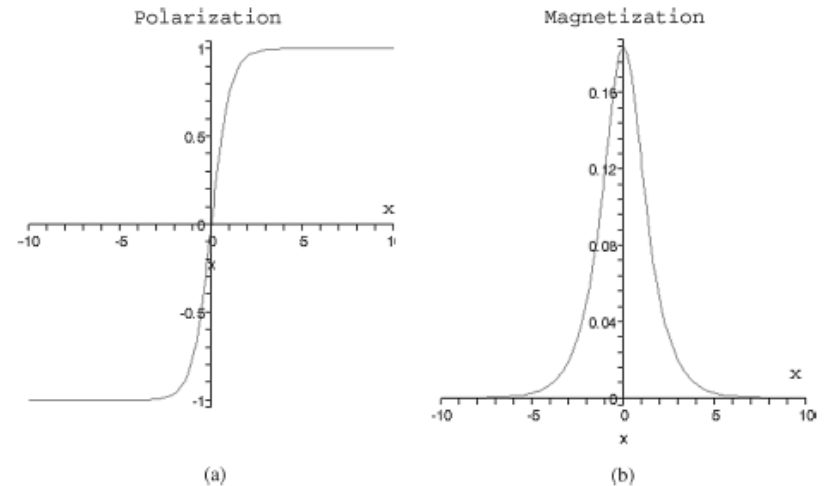


Figure 3. Shape of the ferroelectric polarization and magnetization across the domain wall. A net magnetization appears in the centre of the domain wall even though the domains themselves are still paramagnetic. (See Color Plate IX)

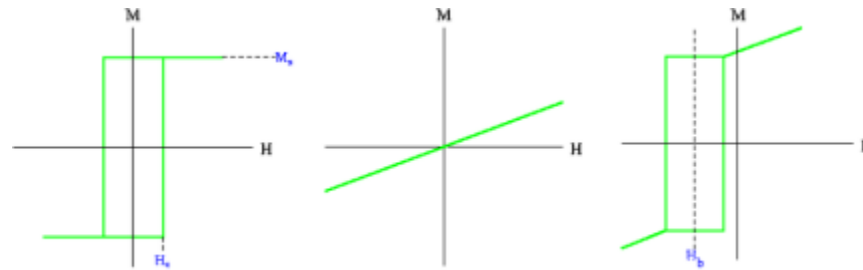
Magnetic Properties

- Magnetoelectric effect

$$P_i = \sum \alpha_{ij} H_j + \sum \beta_{ijk} H_j H_k + \dots$$

$$M_i = \sum \alpha_{ij} E_j + \sum \beta_{ijk} E_j E_k + \dots$$

- Exchange bias



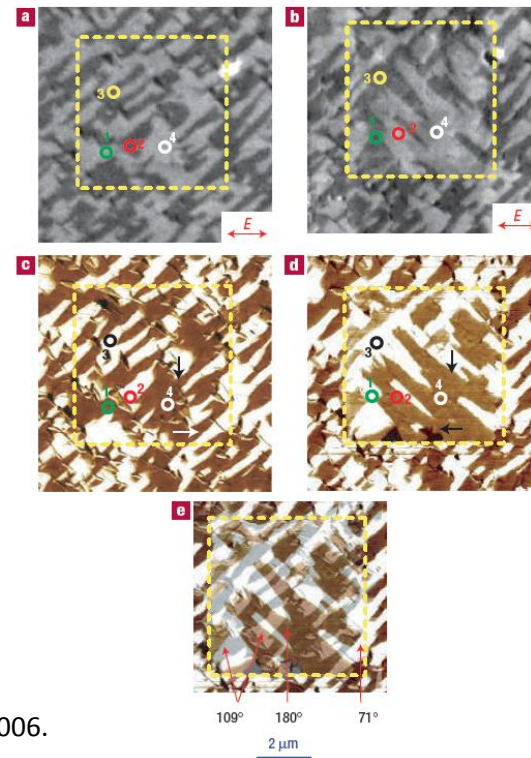
Easy axis magnetization curves of a) Soft ferromagnet

b) Antiferromagnet

c) Exchange biased bilayer

Magnetoelectric effect in BFO

- Coupling between the ferroelectric and antiferromagnetic domains via ferroelasticity



Zhao et al. *Nat. Mater.* 5, 2006.

Figure 5 PEEM and in-plane PFM images of the same area of a BiFeO_3 film before and after electrical poling. a,b, PEEM images before (a) and after (b) poling. The arrows show the X-ray polarization direction during the measurements. c,d, In-plane PFM images before (c) and after (d) poling. The arrows show the direction of the in-plane component of ferroelectric polarization. Regions 1 and 2 (marked with green and red circles, respectively) correspond to 109° ferroelectric switching, whereas 3 (black and yellow circles) and 4 (white circles) correspond to 71° and 180° switching, respectively. In regions 1 and 2 the PEEM contrast reverses after electrical poling. e, A superposition of in-plane PFM scans shown in c and d used to identify the different switching mechanisms that appear with different colours and are labelled in the figure.

Exchange coupling in BFO heterostructures

APPLIED PHYSICS LETTERS 89, 242114 (2006)

Tunnel magnetoresistance and robust room temperature exchange bias with multiferroic BiFeO₃ epitaxial thin films

H. Béa¹⁾
 Unité Mixte de Physique CNRS-Thales and Université Paris-Sud XI, RD 128, 91767 Palaiseau, France
 M. Bibes
 Institut d'Electronique Fondamentale, CNRS, Université Paris-Sud, 91405 Orsay, France

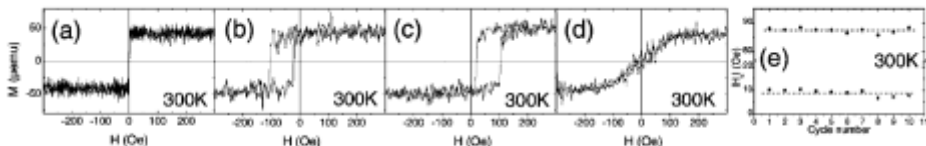


FIG. 4. (a) Hysteresis loop along the [100] direction of CoFeB (5 nm)/Si layer. Hysteresis loops along (b) the [100] direction, (c) the [-100] direction, and (d) the [010] direction of CoFeB (5 nm)/BFO (35 nm)/STO bilayer. (e) Coercive fields of a similar sample for successive H cycles (up to ± 300 Oe). Dashed lines are guides to the eyes.

CoFe/Si and CoFe/BFO/STO/Si

APPLIED PHYSICS LETTERS 91, 172513 (2007)

Room temperature exchange bias and spin valves based on BiFeO₃/SrRuO₃/SrTiO₃/Si (001) heterostructures

Lane W. Martin,^{a)} Ying-Hao Chu, Qian Zhan, and R. Ramesh
 Departments of Materials Science and Engineering and Physics, University of California, Berkeley
 and Materials Science Division, Lawrence Berkeley National Laboratory, Berkeley, California 94720, USA

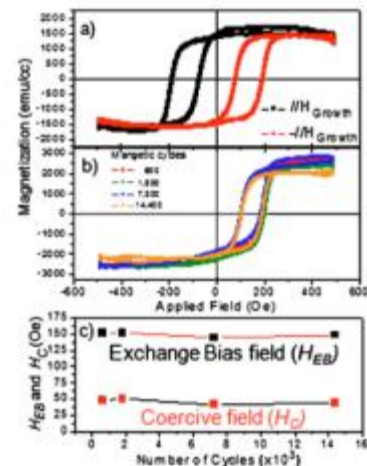
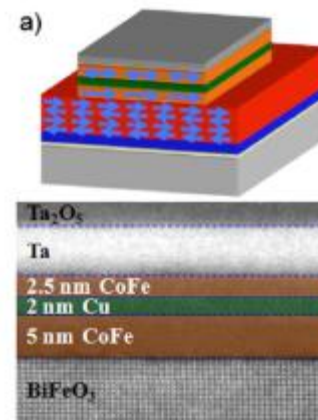


FIG. 5. (Color online) Typical magnetic properties for bilayer CoFe/BFO heterostructures. (a) Magnetization hysteresis loops reveal large negative exchange bias. (b) Repeated magnetic cycling results in very little change in the magnetic properties. (c) Exchange bias field and coercive field as a function of magnetic cycle—no training effect is observed.



Nanoscale Control of Exchange Bias with BiFeO₃ Thin Films

Lane W. Martin,^{*,†,‡} Ying-Hao Chu,^{†,§,||} Mikel B. Holcomb,^{†,§} Mark Huijben,[§] Pu Yu,[§] Shu-Jen Han,^{||} Donkoun Lee,^{||} Shan X. Wang,^{||} and R. Ramesh^{†,§}

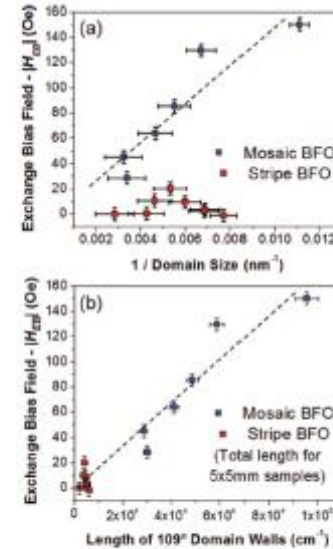
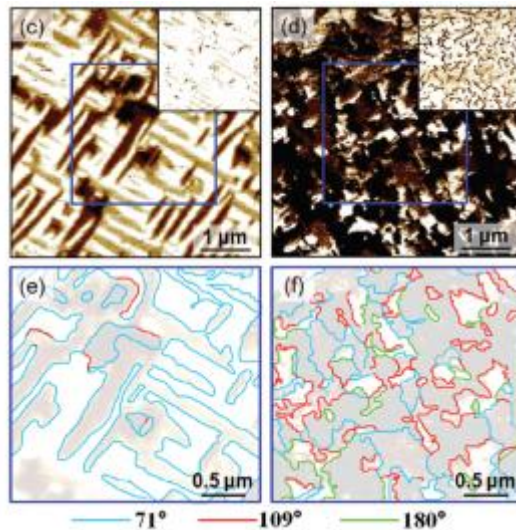
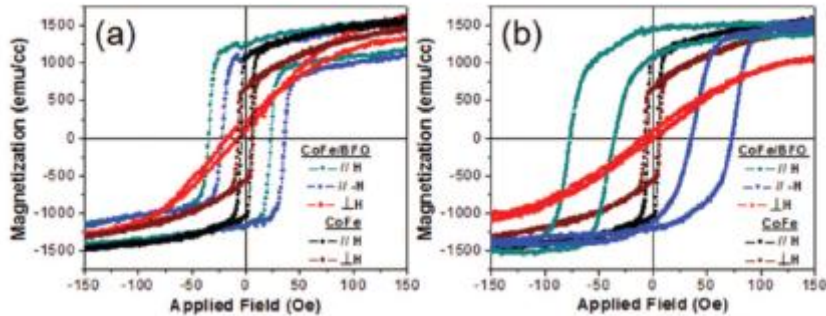


Figure 2. (a) Dependence of exchange bias field on domain size for CoFe/BFO heterostructures grown on mosaic-like (blue) and stripe-like (red) BFO films. (b) Exchange bias field of the same samples here graphed as a function of the total length of 109° domain walls/sample surface area in 5 × 5 mm samples.

- 109° DWs are influential
- Might be the origin of uncompensated spin at the surface

How to make more functional?

- Electrical control of Ferromagnetic layers by exchange coupling

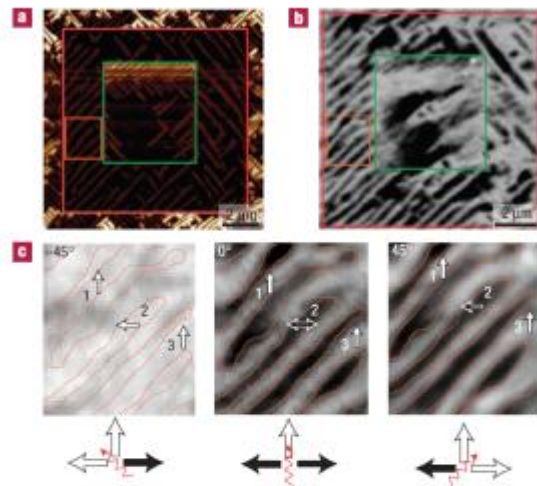


Figure 3 Microscopic evidence for coupling. **a**, In-plane PFM image showing the ferroelectric domain structure of a BFO film with a large (10 μm , red square) and small (5 μm , green square) electrically switched region. **b**, Corresponding XMCD-PEEM image taken at the Co L-edge for a CoFe film grown on the written pattern. Direct matching of domain structures is evident. Black contrast is interpreted as a spin pointing side-to-side in the image and grey as spin pointing up. **c**, Rotation of the sample in reference to the incoming right-circularly polarized light enables full determination of the nature of magnetism in the CoFe layer.

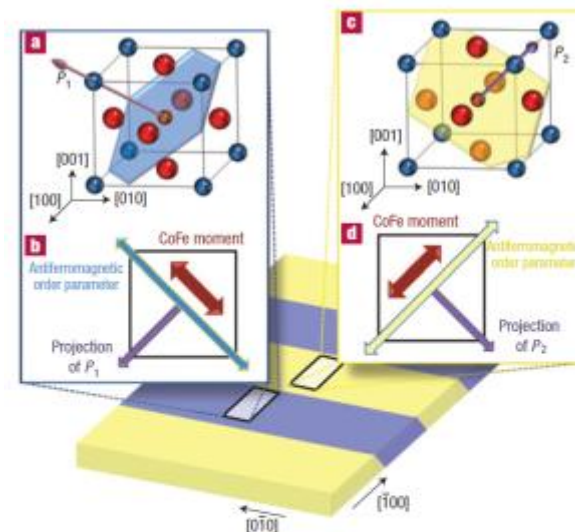


Figure 4 Mechanism of coupling in CoFe/BFO heterostructures. **a-d**, Schematic diagrams of two adjacent domains in the [001]-oriented BFO crystal (**a,c**), in which the [111] polarization directions as well as the antiferromagnetic plane (that is perpendicular to this P direction) are identified, and the corresponding projections of the polarization direction, the antiferromagnetic plane onto the [001] and the corresponding M -directions in the CoFe layer (**b,d**).

ARTICLES

Electric-field control of local ferromagnetism using a magnetoelectric multiferroic

YING-HAO CHU^{1,2,14}, LANE-BE MARTIN^{1,14}, MIKE B. HOLCOMB¹, MATTH GAUS¹, SHU-JEN HANF¹, QIANG HE¹, ANJA BAUK¹, CHAN-HO YANG¹, DANZHEN LIU¹, WEI HEP¹, GUAN ZHAN^{1,1}, FO-LING YANG^{1,2}, ANANTYA FRALÉ-RODRÍGUEZ¹, ANDREAS SCHÖLL¹, SHAN X. WANG¹ AND R. RAMESH^{1,2,3}

¹Department of Materials Science and Engineering, University of California, Berkeley, Berkeley, California 94720, USA

²Department of Physics, University of California, Berkeley, Berkeley, California 94720, USA

³Materials Science Division, Lawrence Berkeley National Laboratory, Berkeley, California 94720, USA

⁴Department of Materials Science and Engineering, National University of Science and Technology, H-10080, Islamabad, Pakistan

⁵Center for Quantum Information Science, Beijing University of Aeronautics and Astronautics, Beijing 100191, China

⁶Department of Materials Science and Engineering, University of California, Berkeley, California 94720, USA

⁷These authors contributed equally to this work

© 2014 ScienceDirect Publishing

How to make more functional?

- Electrical control of Ferromagnetic layers by exchange coupling

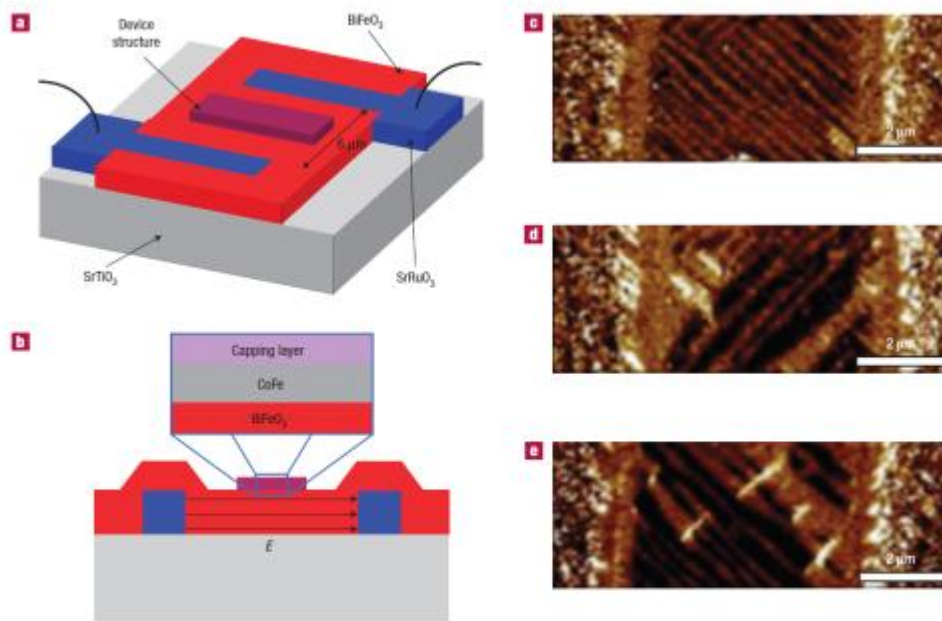


Figure 5 Dynamic switching device structure. **a, b**, Three-dimensional **(a)** and cross-sectional **(b)** schematic diagrams of the coplanar epitaxial electrode device showing the structure that will enable controlled ferroelectric switching and electrical control of local ferromagnetism in the CoFe features. **c-e**, In-plane PFM images showing the ferroelectric domain structure for a device in the as-grown state **(c)**, after the first electrical switch **(d)** and after the second electrical switch **(e)**.

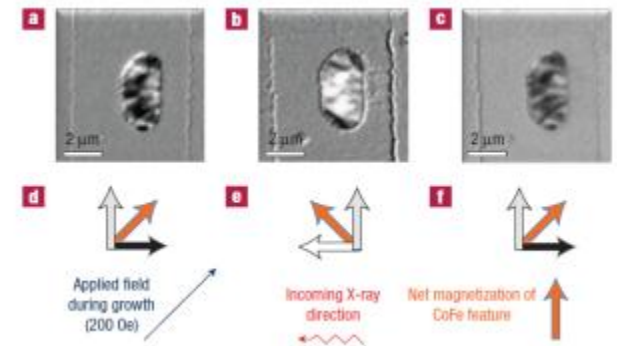


Figure 6 Electrical control of local ferromagnetism. **a-c**, XMCD-PEEM images taken at the Co *L*-edge revealing the ferromagnetic domain structure of the CoFe features in such a coplanar electrode device structure in the as-grown state **(a)**, after the first electrical switch **(b)** and after the second electrical switch **(c)**. **d-f**, Schematic descriptions of the observed magnetic contrast (grey, black and white) in the corresponding XMCD-PEEM images, respectively. Application of an electric field is found to rotate the next magnetization of the structures by 90°. The direction of the applied growth field and the incoming X-ray direction are labelled as well.

Device Applications

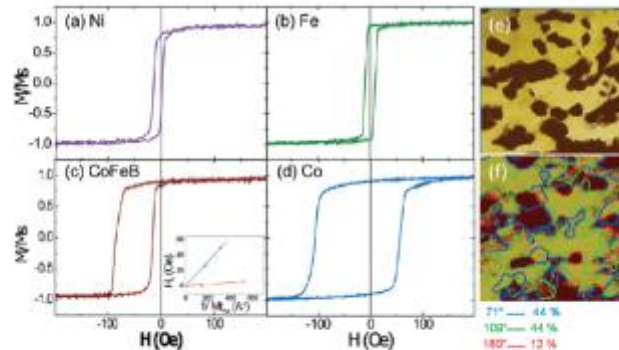


Figure 1. (a–d) Exchange bias for different 4 nm FM/BFO/BFO-Mn samples. Typical out-of-plane (e) and in-plane (f) PFM images of ferroelectric domain patterns and DW analysis of the BFO-Mn/BFO bilayer. The scan area is $1 \times 1 \mu\text{m}^2$. Inset: corresponding evolution of the exchange bias as a function of $1/M_{tBFO}$.

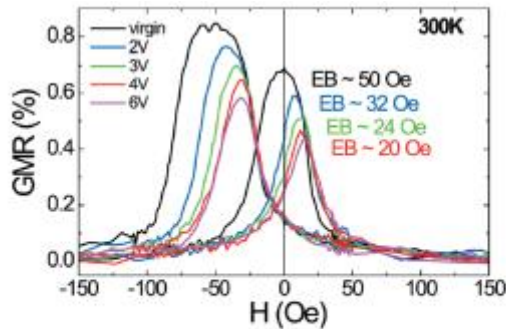


Figure 3. (a) GMR curves of a Au 6 nm/Co 4 nm/Cu 4 nm/CoFeB 4 nm spin valve after different poling events applied to the BFO/BFO-Mn bilayer. The stripe is $210 \mu\text{m}$ long and $20 \mu\text{m}$ wide.

Room Temperature Electrical Manipulation of Giant Magnetoresistance in Spin Valves Exchange-Biased with BiFeO₃

Jule Allibe,¹ Stéphane Fusil,^{1,2} Karim Bouzehouane,¹ Christophe Daudmont,¹ Daniel Sando,¹ Eric Jacquet,¹ Cyrille Deranlot,¹ Mamef Bibes,¹ and Agnès Barthélémy^{1,1}

¹Unité Mixte de Physique CNRS/Thales, 1 Av. A. Fresnel, Campus de l'École Polytechnique, 91127 Palaiseau, France, and Université Paris-Saclay, 91405 Orsay, France

²Université d'Evry-Val d'Essonne, Bd. F. Mitterrand, 91025 Evry cedex, France

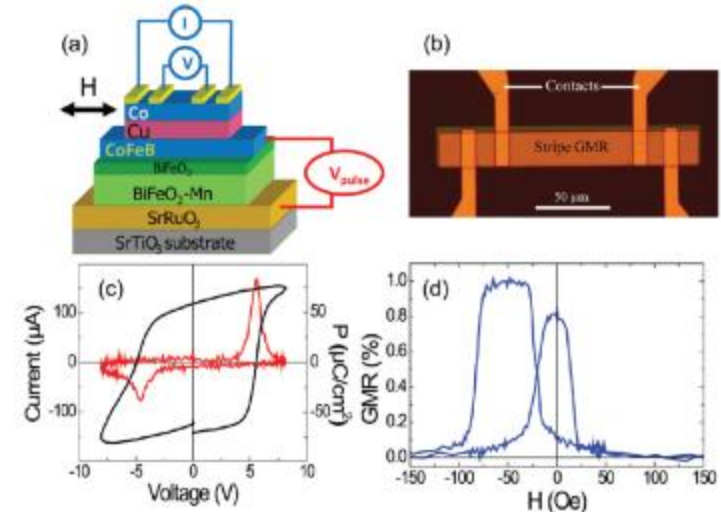


Figure 2. (a) Schematic of the device, (b) micrograph of the stripes with the electrical contacts, and (c) current and polarization versus electric field for a BFO/BFO-Mn bilayer. (d) Giant magnetoresistance of a Au 6 nm/Co 4 nm/Cu 4 nm/CoFeB 4 nm spin valve after patterning ($30 \times 185 \mu\text{m}^2$ stripe).

Conclusions and Outlook

- Exchange coupling mechanism to be investigated more
- Possibility of BFO to be implemented in spintronics devices
- Increasing the efficiency of devices

References

- Wang et al. “Epitaxial BiFeO₃ Multiferroic Thin Film Heterostructures” *Science* **299**, 1719 (2003)
- Eerenstein et al. “Comment on Epitaxial BiFeO₃ Multiferroic Thin Film Heterostructures” *Science* **307**, 1203 (2005)
- Daraktchiev et al. “Landau Theory of Ferroelectric Domain Walls in Magnetoelectrics” *Ferroelectrics* **375**, 122 (2008)
- Zhao et al. “Electrical Control of Antiferromagnetic Domains in Multiferroic BiFeO₃ films at Room Temperature” *Nat. Mater.* **5**, 823 (2006)
- Béa et al. “Tunnel Magnetoresistance and Robust Room Temperature Exchange Bias with Multiferroic BiFeO₃ Epitaxial Thin Films” *Appl. Phys. Lett.* **89**, 242114 (2006)
- Martin et al. “Room temperature exchange bias and spin valves based on BiFeO₃/SrRuO₃/SrTiO₃/Si (001) heterostructures” *Appl. Phys. Lett.* **91**, 172513 (2007)
- Martin et al. “Nanoscale Control of Exchange Bias with BiFeO₃ Thin Films” *Nano Letters* **8**, 2050 (2008)
- Chu et al. “Electric field control of local ferromagnetism using a magnetoelectric multiferroic” *Nat. Mater.* **7**, 478 (2008)
- Allibe et al. “Room Temperature Electrical Manipulation of Giant Magnetoresistance in Spin Valves Exchange-Biased with BiFeO₃” *Nano Letters* **12**, 1141 (2012)